Shahid Bahonar University of Kerman

Biomechanism and Bioenergy Research

Online ISSN: 2821-1855
Homepage: https://bbr.uk.ac.ir

Iranian Society of Agricultural Machinery Engineering and Mechanization

Development of a Guidance System for an Agricultural Wheeled Robotic Platform in Row Crop Fields

Hossein Behfar[1]✉, Fahime Hashemi[1], Arezu Nobakht[1]

[1] Biosystem Mechanical Engineering Department, Faculty of Agriculture, Tabriz University, Tabriz, Iran.

✉ Corresponding author: behfar@tabrizu.ac.ir

ARTICLE INFO

Article type:

Research Article

Article history:

Received 23 October 2023

Received in revised form 28 March 2024

Accepted 30 May 2024

Available Online 30 June 2024

Keywords:

Robotic Platform, Vision-Based Navigation, Differential Steering, Pulse Width Modulation (PWM), Crop Row Detection.

ABSTRACT

Smart and precision agriculture seeks to boost the efficiency of operations and crop yield by using modern technology. Modern tools such as sensors, imagery cameras, and deep learning enable farmers to identify and control weeds, pests, and diseases in real-time. A robotic platform can carry these modern types of equipment and achieve the mentioned objectives precisely. Automatic and accurate navigation of this autonomous robot in agricultural fields is essential for performing these precision tasks. An agricultural robotic platform was designed and developed for row crop fields. The robot navigation system comprises two main components: a vision-based row detection system for path tracking and a motion controller system. The vision-based guidance system processes acquired image data from a tilted camera in front of the robot to identify the crop row's position. The Hough transform method was used to determine the position of the crop rows. Using the resultant guidance line equations, the motion controller directs the robot to move automatically between rows without harming the crops. Differential speed steering allows both wheels on the robot to rotate at different speeds. The steering system improved the robot position error by controlling both powered wheel speeds. To move the robot among the crop rows, it generates the wheel speed difference command. The robotic platform effectively followed the rows of sugar beets at a velocity of 0.5 m/s, exhibiting an average lateral offset of 12 mm and a standard deviation of 22 mm.

Cite this article: Behfar, H., Hashemi, F., & Nobakht, A. (2024). Development of a Guidance System for an Agricultural Wheeled Robotic Platform in Row Crop Fields. *Biomechanism and Bioenergy Research*, *3*(1), 14-25. https://doi.org/ 10.22103/BBR.2024.22392.1063

Publisher: Shahid Bahonar University of Kerman
DOI: https://doi.org/ 10.22103/BBR.2024.22392.1063

NTRODUCTION

Increasing crop yield is the most effective way to address the current food production problem worldwide. Precision agriculture technology can help achieve this goal by using modern site-specific crop management methods and tools. Precision agriculture involves the application of the right amount of inputs at the right time and place to improve crop productivity and yield. However, conventional tractors used in agricultural practices face challenges in meeting the precision requirements of modern farming systems. These tractors are limited in maneuverability and precise control, and their heavy weight can cause soil compaction. While most tractors use a mechanical steering system, precise electronic steering control is either not feasible or expensive (Jurik & Zhang, 1999). As a result, farmers had to employ laborers for their precision agricultural tasks like inter and intra-row weeding management (Zhang et al., 2022).

Due to the COVID-19 pandemic and other infections, temporary labor shortages are affecting productivity worldwide. As a result, farmers are exploring new ways to automate their farming operations and reduce the need for human intervention. Mobile robots are becoming increasingly important in this regard because they can carry out precision tasks on farms with greater accuracy and precision than tractors. Additionally, small and lightweight robots can minimize the risk of soil compaction and environmental impact. With new sensors such as vision cameras and GPS technologies, these robots offer high maneuverability and precise control, making them a flexible platform for precision farming applications. They are particularly beneficial for automating tasks such as precision planting, weeding, spraying, fertilization, phenotyping, harvesting specific crops, and creating datasets required for machine learning (Mueller-Sim et al., 2017). However, high-precision guidance remains a significant challenge for agricultural systems using these robots.

On-site robot guidance can be accomplished by using two methods: machine vision and a high-precision global positioning system equipped with DGPS or RTK. Weed control robots were first presented in 2002 by Astrand and Baerveldt (2002) and Blasco et al. (2002). They used mechanical actuators and selective high-voltage electric discharge to remove the weed.

Astrand and Baerveldt (2002) developed their robot at Halmstad University in Sweden. It had a length of 120 cm and a width of 70 cm and was designed for row crops with a row spacing of 50 cm. Its steering system was controlled by a servomotor and was guided by an image processing system to follow rows of sugar beet crops. Bak and Jacobsen (2004) constructed a robot for farming in Denmark. The robot was used for monitoring and mapping weed density. The machine vision system detected crop rows and guided the robot between rows at 25 and 50 cm row intervals. This robot, called the robotic platform, had four moving wheels with electric motors. The system had a standard deviation of 1-1.6 cm at a low speed of 0.2 m/s. This error increased to 7.10-7.7 cm at high speed of 1.6 m/s. A robot for weeding was developed by Baker et al. (2010) at Wageningen University in the Netherlands for weeding. This robot was the only farm robot that was fully hydraulic. The drive system was powered by a 31.3 kW diesel engine, unlike most of the current new robots. The system failed to become commercial due to issues such as environmental pollution and vibrations, which are commonly faced by combustion engines. This system was controlled simultaneously by RTK GPS (absolute positioning), machine vision, and Dead Reckoning (relative positioning) technologies. The maximum error and deviation from its row was 3 cm at the speed of 0.5 m/s with a standard deviation of 1.2 cm. Dong et al. (2011) developed a robotic system for harvesting white asparagus. It had a length of about 3 meters, weighed 450 kg, and was able to harvest asparagus automatically at a crop row distance of 0.8 m with a height of about 0.5 m. The image processing system has completed the task of

detecting rows. The electric motors that powered its two driving wheels had a power of 450 W with a nominal torque of 12.6 Nm. Bowden et al. (2014) at the University of Queensland, Australia, developed a compact SRVF all-purpose agricultural robot. It was a four-wheeled robot with two driven wheels and a differential steering system. The robot's length was 3 meters and its width was 2.5 meters. This device was capable of reaching speeds of up to 1.4 m/s (5 km/h) and produced a maximum power of 5.4 kW. Grimstad and Fram (2017) developed the Thorvald series of agricultural robots in Saga Robotics, which were modular. The assembly was determined by their application in the field or greenhouse and the type of operation. Yanmar Inc. has presented four models of robots) in Italy, including Agrobot (unmanned ground robot), Platoid (soil conditioning robot), Flybot (drone), and Ankillarybot (service robot in open areas. The spatial accuracy of the Agrobot was ±0.02 meters due to its RTK GPS position control system. The guidance was provided by vision and laser sensors. The vision system had RGB and stereo color systems installed (Sarri et al., 2020). A wheeled robot consists of several main components, such as the chassis, the drive system (power generation), the guidance and control system, the steering system, and the agricultural equipment (e.g., a weeding unit) (Bechar & Vigneault, 2016). Vision based guidance is usually performed for row detection (Marchant & Brivot, 1995).

Row detection based on image processing

To begin with vision based row detection, the image pixels that are associated with plants need to be identified and separated several methods have been suggested to differentiate the pixels associated with the green portions of plants. Marchant and Brivot (1996). Tillet et al. (2002), and Astrand and Baerveldt (2002) used a band pass filter to block visible wavelengths in images acquired by a CCD monochrome camera to enhance plant segments in near-infrared. Meanwhile, Bakker et al. (2008) improved the contrast between the background and plants by combining normalized color channels and transforming them into a grayscale image.

Segmentation, as the second step, is typically performed by thresholding in row detection. After carrying out the necessary steps to obtain thresholded images, row detection algorithm as the third step should be applied. Vision-based row detection algorithms are divided into two categories: traditional and machine learning methods (Shi et al., 2023). These are stripe analysis, stereo-vision, blob analysis, linear regression, and Hough transform (Bai et al., 2023).

The horizontal strips method involves dividing the images into horizontal strips and calculating the center of gravity of each row section. Points are then marked in each strip to indicate these centers of gravity. By joining these points, the lines of the rows can be obtained (Hague & Tillett, 2001; Sainz-Costa et al., 2011; Søgaard & Olsen, 2003).

In blob analysis-based row detection, the main blobs are formed by attaching adjacent pixels with the same value in segmented images. For a blob to be considered as a main blob, it should have a minimum sum of 200 pixels. The center of gravity and the angle of the primary axes of the main blobs are then calculated (Fontaine & Crowe, 2006).

Stereo-vision processing involves the acquisition of 3D coordinates for ROI points from stereo images using a pair of cameras. To ensure accurate application of this method, the crops must meet a minimum height requirement (Kise et al., 2005; Rovira-Más et al., 2008).

The Hough transform is a widely used algorithm for detecting rows in classic row detection (Shi et al., 2023). The specifics of the method are elucidated in the subsequent section. Astrand and Baerveldt (2002) and Bakker et al. (2008) utilized the Hough transform on segmented images of sugar beets. Van Evert et al. (2006), Bonadies et al. (2019) and García-Santillán et al. (2018) employed this transform method for corn, lettuce, and potato fields, respectively. Choi et al. (2015) utilized the Hough transform on selected leaves of rice plants, which were chosen based on morphological

image processing. Bejay et al. (2023) implemented a fusion of the Hough transform and Lidar sensor to navigate their field robot. Chen et al. (2021) applied the Hough transform to process images captured by unmanned aerial vehicles (UAV).

A variety of test and field robotic platforms equipped with electric motors have been successfully developed by the Biosystem Engineering Department at the University of Tabriz (the laboratory of electrical and instrumentation systems). This was done to take advantage of the many benefits of electric robots, such as their lack of vibration, high control accuracy, ability to prevent pollution, simple power transmission system, and easy controllability (Kamandar et al., 2022). The research focused on developing a robot guidance system, which consisted of two parts: a machine vision-based row detection system and a guidance system.

MATERIALS AND METHODS

The first platform was moved by an AC motor-driven winch on a rail that was powered by an inverter and was situated next to a soil bin. The length of the cultivation soil bin was 7 meters (as shown in Figure 1-a). The tools being considered were attached to the test platform and evaluated. The chosen tool was then installed on a mobile field robot for further testing in the field. The dimensions of the mobile platform were the same as those of the mobile-wheeled robot (Figure 1-b).

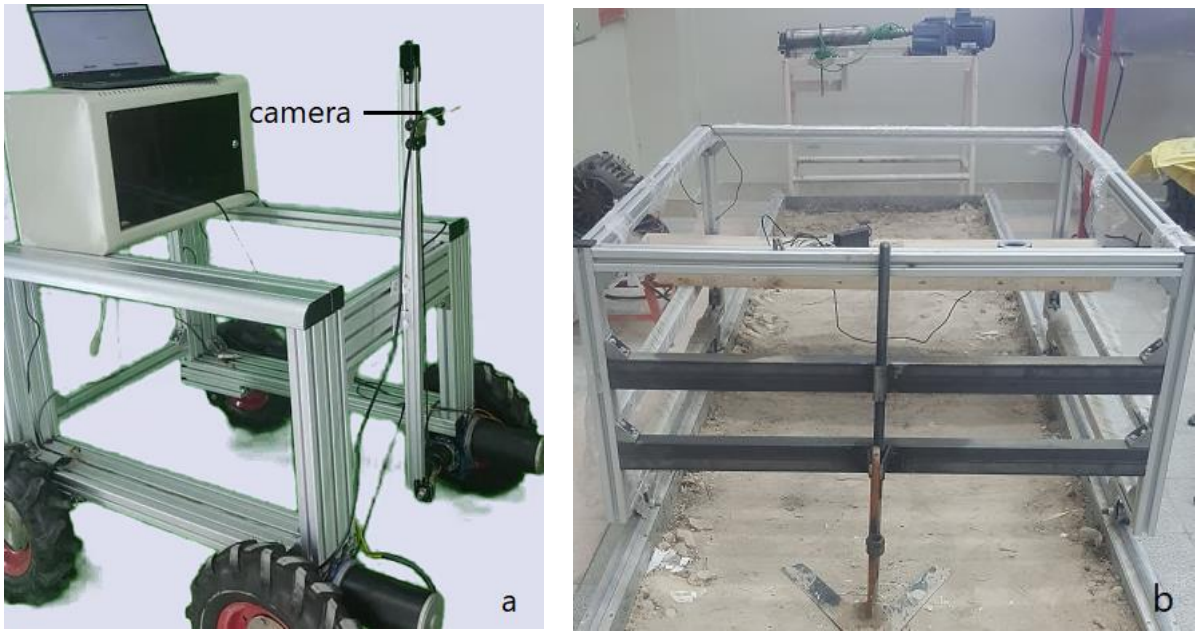

Figure1. a: field platform b: laboratory platform

The platform overview

The robot is an all-electric, lightweight robotic platform that can be controlled in two ways, including manual control and automatic guidance. The robotic system includes a modular chassis, vision system, driving unit and its control circuit, power supply, and steering system. The track width of the robot is 1000 mm. The platform chassis width and length is 800 mm and 1000 mm, respectively. It was initially designed to work on sugar beet and maize farms with row distances of 500 mm and 750 mm respectively. The robot passes above two rows of sugar beets and one row of maize crops, which are located between the wheels. The wheels were placed 25 cm and 15 cm apart from the planting row in sugar beet and maize fields respectively, to prevent damage to the crops.

One of the key features of the robot is its modular configuration for various operations, achieved through its engineering grooved profile units. The side view of the robot structure in Figure 1-b shows two completely independent side units beside the wheels. The robot's height can be adjusted to suit crops with different sizes. The side units contain all the primary drive components, such as gearbox, wheels, motors, batteries, etc. The span between them is a clear, open space without any main components. Several transverse profiles connect the side units, making it easy to adjust the robot's width based on the distance between the rows.

The enclosed workspace between the chassis, measuring 800×1000×700 mm^3, is used for weed or crop detection. A downward-facing camera and lighting system can be mounted above this area. The manipulator, such as Cartesian arms or implement units like spot spraying or selective hoe can be mounted at the rear profile that connects the two side units.

The robot's driving system has two passive wheels and two active wheels, which enable it to move around. The wheels have a diameter of 400 mm, and the robot has two batteries located at the center of each side unit. These rechargeable batteries have a capacity of 60 amp-hours and output 12 volts of power. They are connected in series to provide a 24-volt supply, which allows the robot to operate for three to four hours.

To provide the robot with a speed of up to 1 m/s, two 500W DC motors were used, each with a maximum rotation speed of 2500 at 24V. They were combined with 50:1 gearboxes. There are also two encoders mounted on each wheel shaft that sense the robot's displacement and speed (Figure 2). They provide feedback signals for speed control. Rotary encoders count the number of pulses for each wheel rotation, which has a resolution of 2500 pulses per revolution. This means they can measure 0.5mm of displacement per pulse.

Figure 2. Encoder

Image processing based row detection

The choice of machine vision for robot navigation was made due to the limitations of DGPS service and expensive RTK-GPS systems in Iran. The guidance system is responsible for controlling the position of the robot to follow a crop row. To achieve this, the system relies on a vision system that calculates the offset and heading error of the robot at the front relative to the rows. The image processing algorithm for crop row recognition then calculates the distance of the closest row from the robot's center at the nearest horizontal line to the robot chassis, the heading angle of the row line at this horizontal border, and the time it takes to process this information.

Two types of cameras was tested in the guidance system: Basler camera acA-1920 with a resolution of 1920 × 1080 pixels and acA1300-60gmNIR. The first one provides a color output in three channels (R, G, and B), the second one has a single gray channel output. The camera is mounted at the front of the vehicle, facing downward to capture images of rows. The camera height from the ground and its tilted angle depends on the plant's growing period. The smaller the crop's size, the lower the camera height, and the wider the camera angle (relative to the perpendicular to the ground). The camera angle is changed by a servo motor. The camera was mounted at about 100mm above the ground level tilted downward, looking forward at an angle of about 45 degrees (Figure 1.a).

It was expected that the green channel values would be used for image segmentation due to the green color of plants. However, the row detection algorithm had to be robust to variable field

conditions. Variability arises from changes in row geometry, plant height and size, weed infestation, natural lighting, partially missing plants, and objects' presence such as stones and crop residues. These issues were considered in the processing code, and therefore a combination of color channels such as 2*(green) - red - blue was used instead of the green value.

The thresholding operation was used to separate the pixels of the plant from the soil. The line equation was then obtained through the Hough method, and the amount of deviation from the path was calculated. In the Hough transform, the position (x, y) of pixels related to the plant was converted to polar space in terms of (ρ, θ), by using the equation of 1.

$$\rho = x\cos\theta + y\sin\theta \quad (1)$$

Where, ρ is normal distance from origin and θ is the angle of this line with horizental line.

In this space, a sine curve was drawn for each point (Figure 3-a). The polar coordinate axis space is divided into cells, and the accumulators of these cells count the number of sinusoidal curves that pass through each one. The accumulators with the most passes (brighter points in Figure 3-a) are the main line coordinates in polar form. These coordinates show the normal distance from the origin and the angle of the normal line of the row line. By using some geometric relationships, the robot offset and heading angle were calculated. To digitize the values, the space was given a resolution value (resolution), which was usually 0.2 degrees for the angle and 1 cm for the width from the origin

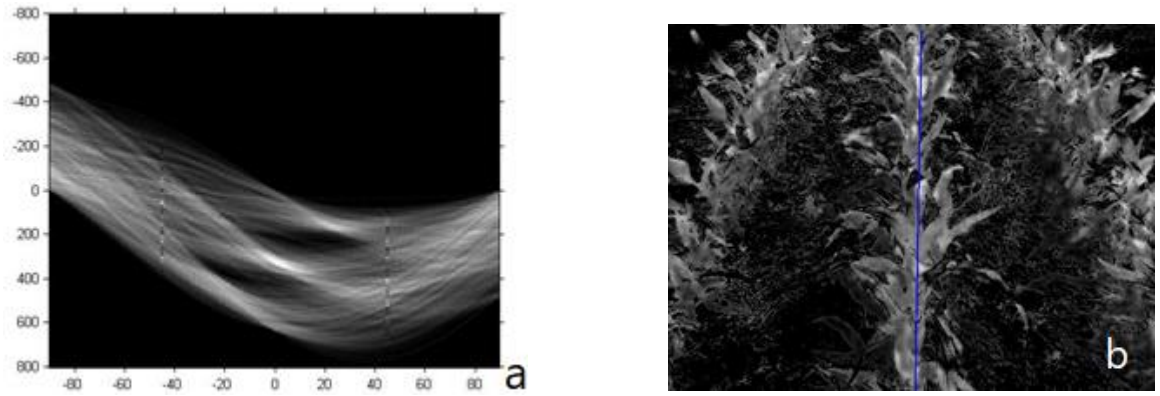

Figure 3. a: Hough space b: detected line for a row

The steering system

The second main objective of this research was to develop an interface circuit between the computer and the motors to receive signals through the vision system. This circuit performs two main tasks. First, it transmits a signal from the digital system with low power to the motor system with high power, or in other words, it performs power amplification. Secondly, it creates a safety system to prevent any induced magnetic field or noise from being transmitted from the motors to the control circuit and computer.

This robotic platform is entirely electric and can be easily controlled through signals from the computer control system. The feedback speed control circuit aims to enable automatic tire rotation adjustment to maintain a desired speed and establish the required wheels' difference. Two manual switches provide two different modes: manual and automatic guidance. The robot is transported from the hangar to the field using a manual steering system. There are eight relays available that allow for manual control in

either the forward or backward direction. The system controller interface is an Arduino Mega 2560, which operates both the relays and the speed control.

The robotic platform uses a two-wheel steering mechanism. It utilizes Pulse-Width-Modulation (PWM) output of the Arduino for speed control. The electric power for each motor is supplied through a transistor H-bridge circuit. This circuit not only modifies the applied voltage to change the forward speed but also allows independent speed control for each wheel. Mobile robots based on independent steering wheels offer more benefits, including adaptability to different crops, maneuverability, and adaptability to terrain.

To maintain its position along the crop rows, the robot must move sideways in relation to the rows to correct for any steering errors detected by the computer vision sensor. This is achieved by making a quick turn, which requires adjusting the linear speeds of the left and right wheels. In Figure 4, L represents the distance between the front and rear wheels, W represents the distance between the left and right tires (wheelbase), v_R the linear speed of the right wheel, v_L is the linear speed of the left wheel, and R_O is the rotation radius of the robot. The difference in wheel speeds determines the turning radius, and choosing the right radius is crucial. If the wheel speeds are the same, the turning radius will be infinite, and if one wheel stops moving (skid mode), the turning radius will be zero (in situ rotation). It is recommended that the value of R_O should not be less than the wheelbase, which varies depending on the type of soil. Low values of R_O require a greater difference in angular velocity, which can cause slippage. Additionally, lower voltages must be applied, resulting in reduced power. The recommended value of R_O for agricultural soils is 5-8 meters (Wu et al., 2013).

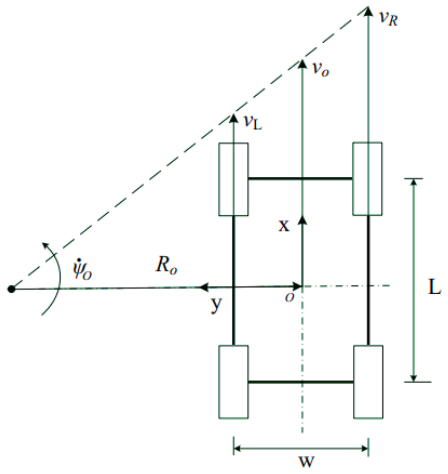

Figure 4. Kinematic model of electric robot with differential steering

Experimental curves were utilized to determine the optimal R_O value. These curves vary according to the forward speed at which the robot operates. Therefore, a specific speed needs to be considered first. The typical speed for robots that perform precise operations such as spot spraying or inter-row weeding is between 0.5-1 m/s. Robots used for in-row cultivation or planting generally have a speed range of 1-5 m/s. The motor and gearbox of the developed robot were chosen to provide a speed of 1 m/s, with a wheel radius of r=20 cm and a circumference of 2r, which equals 1.25 m. The nominal speed of the motors was 2500 rpm, and with a 1:50 gearbox, its nominal speed was 50 rpm or 0.83 rps. Therefore, the forward speed of 1.04 m/s was included in the experiments. The angular speed of the wheels required to achieve this speed was 0.13 rad/s .Experimental tests were conducted to obtain the curve of different values of R_O against different values of the angular speed difference of the left and right wheels at this forward speed (Figure 5).

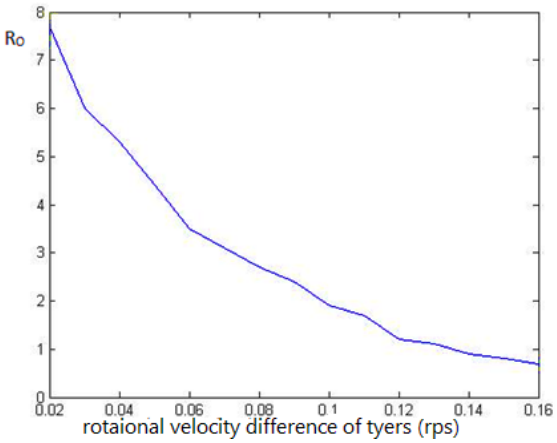

Figure 5. The curve showing the relationship between the angular speed difference of the wheels and the turning radius

When using mobile robots in farms, it is advisable to set the value of R_O between 5 and 8. This is because high rotation angles in farm robots can cause severe slippage, which reduces the efficiency of the system and causes problems with traction. For faster turning, a turning diameter of 5m was chosen. Figure 5 shows an angular speed difference of 0.04 radians/second. In case of excessive slippage, a larger value should be selected.

Applying appropriate voltage to the wheels

A value of R_O 5m was selected for which the angular velocity difference was 0.04 radians/second. The amount of voltage required to generate this angular speed, and hence the numerical value of the PWM required by the controller, was determined in the laboratory. To achieve this, the rotational speed of the wheels and the angular speed were measured for different voltages. Various voltages were created and applied to the motor using the PWM method, and the voltage was read with a voltmeter. The number of revolutions per unit of time (rps) was measured using encoders attached to the wheel (Figure 6).

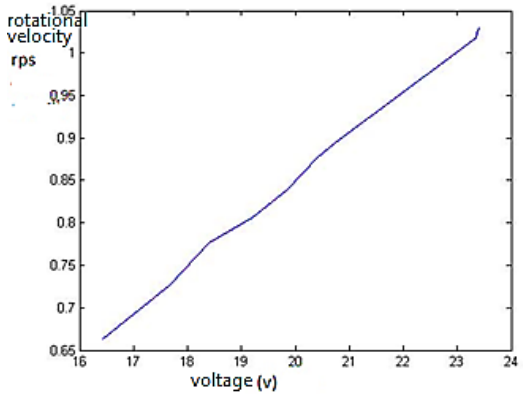

Figure 6. The relationship between voltage and rps

RESULTS AND DISCUSSION

Closed loop control system of the steering camera

In the previous section, we discussed the main feature of this robot, which is the adjustable height and angle of the camera based on the growth stage of the main plant. The camera's height and angle should be adjusted according to the plant's height to ensure accuracy. If the plant is shorter, the camera should be placed lower and its angle should be wider than the perpendicular to the ground. This allows for more continuity between the pixels related to the product row, resulting in a better representation of the row line with higher accuracy as shown in Figure 7-b. If the camera is positioned high and its angle is narrower than the perpendicular direction to the ground, there will be more separation between the green pixels of the row, and the obtained line will not be an ideal representative of the row line, resulting in lower accuracy (Figure 7a)

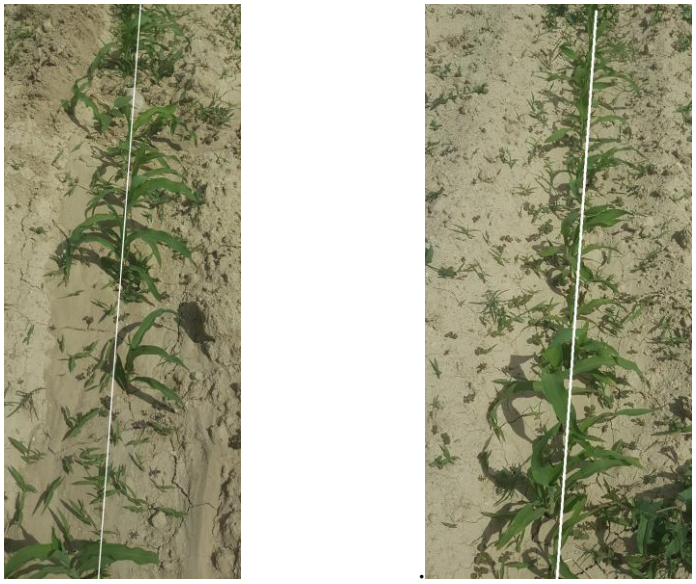

a b

Figure 7. a: Image taken from the row at a lower height b: Image taken from a higher height

The automatic camera control system had a second feature that involved using a light sensor to detect the direction of the sun's radiation. The experiments showed that moving the robot towards the sun during the early hours and late in the day could greatly reduce the accuracy of the system. This was due to the impact of solar rays on the camera sensor and the brightness created on plant leaves, especially sugar beets.

PWM frequency selection for the used motor

The method used to control the speed of the wheels was Pulse Width Modulation (PWM). In the coils, the induction impedance (Z) is directly proportional to the angular speed and the frequency (Relation 2).

$$Z = L\omega j,\ \omega = 2\pi f \qquad (2)$$

Where L is the induction coefficient (with Henry unit).

High Z impedance causes the motor to heat up and reduces the efficiency and life of the motor. Therefore, the value of f should be chosen as a reasonable value. This numerical value should be between 20 and 40 kHz. This value varies from motor to motor, depending on the frequency response of the motor. The dynamic model of a DC motor can be shown in Figure (8). The inductor L is in series with the resistor R. To obtain the transfer function of the motor's electrical system, one must either have access to the values of R and L of the motor or obtain it in the laboratory.

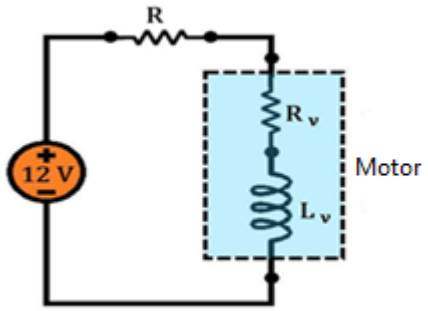

Figure 8. The dynamic figure of the engine used in the design

The manufacturer, Kormas, provided the motor datasheet which contained the necessary information for the laboratory test. To conduct the test, the wire of the motor was connected to a digital voltmeter, and the data collected was recorded on the computer (as shown in Figure 9).

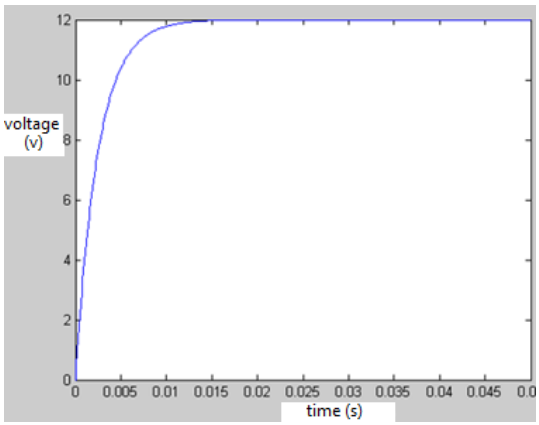

Figure 9. Motor response curve

According to Figure 9, the system becomes stable after 15 ms. Figure 8 shows that the equivalent dynamic system consists of a resistance and an inductor, making it a first-order system. In first-order systems, equilibrium is reached at 5τ, as shown in Figure 10. The time constant of the system (τ) is equal to 3 ms. τ is inversely proportional to the exponential frequency (f), which has a value of 333. The system's function in the time environment is expressed as Relation 3).

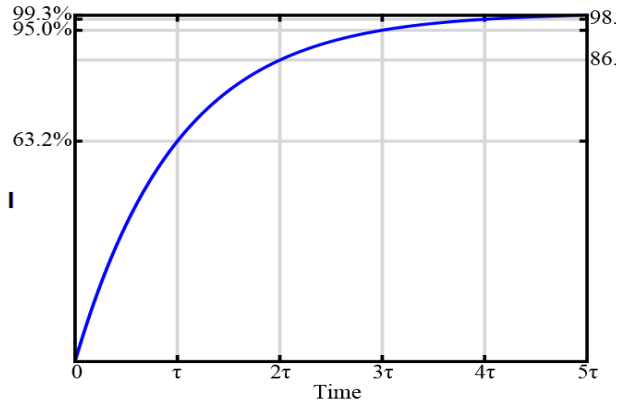

Figure 10. The time constant value of τ

$$V_L=12(1-e^{-333t}) \quad (3)$$

In the design of PWM driver systems, it is recommended to use frequency values higher than the response frequency of the system, i.e. 333. At much higher values, the relationship between current and voltage becomes non-linear. But lower frequencies cause noise. Since the limit of human hearing is 18 Hz, the PWM frequency was chosen higher than 20 kHz. Of course, provided that the frequency creation system can create this frequency.

Steering accuracy of the robotic system

To assess the performance of the robot guidance system and the real-time application of the image processing unit and the row tracking system, a field test was carried out. A powder indicator was used to measure the degree of deviation from the robot's path in the field (Figure 11). The powder was poured in the center of the row.

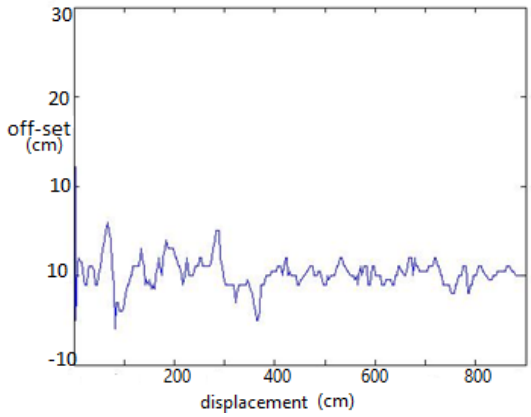

Figure 11. The amount of deviation from the middle line between the rows

The average lateral deviation from the row for the data in Figure 11 was 12 mm. In case of increasing the density of weeds, this error increased up to 25 mm.

CONCLUSIONS

The development of an agricultural robotic platform at the University of Tabriz demonstrates significant advancements in precision farming, particularly for row crop fields. This platform integrates a vision-based row detection system and a motion controller, both essential for the autonomous navigation of the robot between crop rows. The vision-based guidance system leverages image data from a tilted camera and the Hough transform method to accurately identify and track crop rows. This precise tracking allows

the robot to move seamlessly between rows without damaging the crops. Moreover, the differential speed steering system, enhanced by PWM technology, adjusts the side motors' speed, thereby minimizing lateral offset error. The robotic platform exhibited remarkable performance in tracking sugar beet rows with a minimal average lateral offset and standard deviation, showcasing its potential to improve the efficiency and precision of agricultural operations. Overall, the integration of modern technologies in the robotic platform holds promise for advancing smart agriculture by enhancing crop management and operational efficiency.

REFERENCES

Åstrand, B., & Baerveldt, A.-J. (2002). An agricultural mobile robot with vision-based perception for mechanical weed control. *Autonomous robots*, *13*, 21-35. https://doi.org/10.1023/A:1015674004201

Bai, Y., Zhang, B., Xu, N., Zhou, J., Shi, J., & Diao, Z. (2023). Vision-based navigation and guidance for agricultural autonomous vehicles and robots: A review. *Computers and Electronics in Agriculture*, *205*, 107584. https://doi.org/10.1016/j.compag.2022.107584

Bak, T., & Jakobsen, H. (2004). Agricultural robotic platform with four wheel steering for weed detection. *Biosystems Engineering*, *87*(2), 125-136. https://doi.org/10.1016/j.biosystemseng.2003.10.009

Bakker, T., Van Asselt, K., Bontsema, J., Müller, J., & van Straten, G. (2010). A path following algorithm for mobile robots. *Autonomous robots*, *29*, 85-97. https://doi.org/10.1007/s10514-010-9182-3

Bakker, T., Wouters, H., Van Asselt, K., Bontsema, J., Tang, L., Müller, J., & van Straten, G. (2008). A vision based row detection system for sugar beet. *Computers and Electronics in Agriculture*, *60*(1), 87-95. https://doi.org/10.1016/j.compag.2007.07.006

Bawden, O., Ball, D., Kulk, J., Perez, T., & Russell, R. (2014). A lightweight, modular robotic vehicle for the sustainable intensification of agriculture. In *Proceedings of the 16th Australasian Conference on Robotics and Automation 2014* (pp. 1-9). Australian Robotics and Automation Association (ARAA).

Bechar, A., & Vigneault, C. (2016). Agricultural robots for field operations: Concepts and components. *Biosystems Engineering*, *149*, 94-111. https://doi.org/10.1016/j.biosystemseng.2016.06.014

Bijay, R., Amarendra, M., & Asim, D. (2023). Steer guidance of autonomous agricultural robot based on pure pursuit algorithm and LiDAR based vector field histogram. *Journal of Applied Science and Engineering*, *26*(10), 1363-1372.

Blasco, J., Aleixos, N., Roger, J., Rabatel, G., & Moltó, E. (2002). Robotic weed control using machine vision. *Biosystems Engineering*, *83*(2), 149-157. https://doi.org/10.1006/bioe.2002.0109

Bonadies, S., & Gadsden, S. A. (2019). An overview of autonomous crop row navigation strategies for unmanned ground vehicles. *Engineering in Agriculture, Environment and Food*, *12*(1), 24-31. https://doi.org/10.1016/j.eaef.2018.09.001

Chen, P., Ma, X., Wang, F., & Li, J. (2021). A new method for crop row detection using unmanned aerial vehicle images. *Remote Sensing*, *13*(17), 3526. https://doi.org/10.3390/rs13173526

Choi, K. H., Han, S. K., Han, S. H., Park, K.-H., Kim, K.-S., & Kim, S. (2015). Morphology-based guidance line extraction for an autonomous weeding robot in paddy fields. *Computers and Electronics in Agriculture*, *113*, 266-274. https://doi.org/10.1016/j.compag.2015.02.014

Dong, F., Heinemann, W., & Kasper, R. (2011). Development of a row guidance system for an autonomous robot for white asparagus harvesting. *Computers and Electronics in Agriculture*, *79*(2), 216-225. https://doi.org/10.1016/j.compag.2011.10.002

Fontaine, V., & Crowe, T. (2006). Development of line-detection algorithms for local positioning in densely seeded crops. *Canadian biosystems engineering*, *48*, 7.

García-Santillán, I., Peluffo-Ordoñez, D., Caranqui, V., Pusdá, M., Garrido, F., & Granda, P. (2018). Computer vision-based method for automatic detection of crop rows in potato fields. In *Proceedings of the International Conference on Information Technology & Systems (ICITS 2018)* (pp. 355-366). Springer International Publishing. https://doi.org/10.1007/978-3-319-73450-7_34

Grimstad, L., & From, P. J. (2017). The Thorvald II agricultural robotic system. *Robotics*, *6*(4), 24. https://doi.org/10.3390/robotics6040024

Hague, T., & Tillett, N. (2001). A bandpass filter-based approach to crop row location and tracking. *Mechatronics*, *11*(1), 1-12. https://doi.org/10.1016/S0957-4158(00)00003-9

Jurik, T. W., & Zhang, S. (1999). Tractor wheel traffic effects on weed emergence in central Iowa. *Weed Technology*, *13*(4), 741-746. https://doi.org/10.1017/S0890037X00042160

Kamandar, M. R., Massah, J., & Khoshnam, F. (2022). Measuring Some Mechanical Properties of Boxwood and Privet Plants by an Izod Impact Tester. *Biomechanism and Bioenergy Research*, *1*(2), 7-12. https://doi.org/10.22103/BBR.2022.20351.1014

Kise, M., Zhang, Q., & Más, F. R. (2005). A stereovision-based crop row detection method for tractor-automated guidance. *Biosystems Engineering*, *90*(4), 357-367. https://doi.org/10.1016/j.biosystemseng.2004.12.008

Marchant, J. A., & Brivot, R. (1995). Real-time tracking of plant rows using a Hough transform. *Real-time imaging*, *1*(5), 363-371. https://doi.org/10.1006/rtim.1995.1036

Mueller-Sim, T., Jenkins, M., Abel, J., & Kantor, G. (2017). The Robotanist: A ground-based agricultural robot for high-throughput crop phenotyping. In *2017 IEEE international conference on robotics and automation (ICRA)* (pp. 3634-3639). IEEE. https://doi.org/10.1109/ICRA.2017.7989418

Rovira-Más, F., Zhang, Q., & Reid, J. F. (2008). Stereo vision three-dimensional terrain maps for precision agriculture. *Computers and Electronics in Agriculture*, *60*(2), 133-143. https://doi.org/10.1016/j.compag.2007.07.007

Sainz-Costa, N., Ribeiro, A., Burgos-Artizzu, X. P., Guijarro, M., & Pajares, G. (2011). Mapping wide row crops with video sequences acquired from a tractor moving at treatment speed. *Sensors*, *11*(7), 7095-7109. https://doi.org/10.3390/s110707095

Sarri, D., Lombardo, S., Lisci, R., De Pascale, V., & Vieri, M. (2020). AgroBot smash a robotic platform for the sustainable precision agriculture. In *Innovative Biosystems Engineering for Sustainable Agriculture, Forestry and Food Production: International Mid-Term Conference 2019 of the Italian Association of Agricultural Engineering (AIIA)* (pp. 793-801). Springer International Publishing. https://doi.org/10.1007/978-3-030-39299-4_85

Shi, J., Bai, Y., Diao, Z., Zhou, J., Yao, X., & Zhang, B. (2023). Row detection BASED navigation and guidance for agricultural robots and autonomous vehicles in row-crop fields: methods and applications. *Agronomy*, *13*(7), 1780. https://doi.org/10.3390/agronomy13071780

Søgaard, H. T., & Olsen, H. J. (2003). Determination of crop rows by image analysis without segmentation. *Computers and Electronics in Agriculture*, *38*(2), 141-158. https://doi.org/10.1016/S0168-1699(02)00140-0

Tillett, N., Hague, T., & Miles, S. (2002). Inter-row vision guidance for mechanical weed control in sugar beet. *Computers and Electronics in Agriculture*, *33*(3), 163-177. https://doi.org/10.1016/S0168-1699(02)00005-4

Van Evert, F. K., Van Der Heijden, G. W., Lotz, L. A., Polder, G., Lamaker, A., De Jong, A., . . . Van Der Zalm, T. (2006). A mobile field robot with vision-based detection of volunteer potato plants in a corn crop. *Weed Technology*, *20*(4), 853-861. https://doi.org/10.1614/WT-05-132.1

Wu, X., Xu, M., & Wang, L. (2013). Differential speed steering control for four-wheel independent driving electric vehicle. In *2013 IEEE International Symposium on Industrial Electronics* (pp. 1-6). IEEE. https://doi.org/10.1109/ISIE.2013.6563667

Zhang, W., Miao, Z., Li, N., He, C., & Sun, T. (2022). Review of current robotic approaches for precision weed management. *Current robotics reports*, *3*(3), 139-151. https://doi.org/10.1007/s43154-022-00086-5